

Dynamical origin of the quantum chaotic motion of a single particle in the two-center shell model

Jian-zhong Gu^{1,2,3}, Yi-zhong Zhuo^{2,4}, En-guang Zhao^{2,3}, Xi-zhen Wu⁴, Hong-shi Zong^{2,3}

¹ CCAST (World Lab.), P. O. Box 8730, Beijing, 100080, P. R. China

² Institute of Theoretical Physics, Academia Sinica, P. O. Box 2735, Beijing, 100080, P. R. China

³ Center of Theoretical Nuclear Physics, National Laboratory of Heavy Ion Accelerator, Lanzhou, 730000, P. R. China

⁴ China Institute of Atomic Energy, P. O. Box 275(18), Beijing, 102413, P. R. China

Received: 27 April 1998 / Revised version: 20 July 1998

Communicated by P. Schuck

Abstract. For the single-particle potential surface of the two-center shell model, two geometrical quantities which determine the local Liapunov exponents are derived. It is shown that the appearance of a large positive local Liapunov exponent in a large area of the coordinate space leads to the quantum chaotic motion of a single particle in heavy nuclei. For both small and large (or medium) separations of the two centers, the dependence of the quantum chaotic motion on the neck deformation is interpreted from the dynamical point of view.

PACS. 05.45.+b Theory and models of chaotic systems – 21.60.Cs Shell model – 03.20.+i Classical mechanics of discrete systems: general mathematical aspects – 11.10.Lm Nonlinear or nonlocal theories and models – 11.30.Na Nonlinear and dynamical symmetries

1 Introduction

One of the best systems for the studies of quantum chaos is the atomic nucleus. Roughly speaking, the studies of quantum chaos related to nuclei have two aspects. One is to discuss the chaos in realistic nuclei [1,2]. The other is to investigate the single-particle (nucleonic) motion in a deformed nucleus based on the mean field approach [3-5]. The symmetry (or absence of symmetry) of the mean field associated with the geometric shape of nuclei determines the regularity (or chaoticity) of the single-particle motion. In our previous work [6], in the framework of the two-center shell model (TCSM) we have systematically studied the nearest neighbor level spacing distribution and spectral rigidity of single-particle energy levels of heavy nuclei when the shape parameters of a nucleus are changed. The shape parameter region, in which the spacing distribution of spectra and spectral rigidity are approximately close to those of the Gaussian orthogonal ensemble (GOE), was found. We call this shape parameter region as the chaotic region of shape parameters, in which the quantum chaotic motion of a single particle is realized. Meanwhile, we have found that there is a good quantum-classical correspondence for the regular (chaotic) single-particle motion [7]. Although the relationship between the quantum chaotic motion and the shape deformation has been clarified, the

dynamical origin of the quantum chaotic motion remains to be an open question.

During the past few decades, there has been increasing interest in the study of the relationship between the local instability governed by geometry of potential energy surface and the global instability of a system. In 1974 Toda [8] considered a periodic lattice of the three particles with nearest neighbour nonlinear interaction and introduced a criterion that a trajectory is stochastic (chaotic) if it passes through regions of the local instability in which the curvature of the potential energy surface has negative value. The criterion has been called often Toda criterion. Toda criterion has been criticized soon after its formulation, e. g. in the paper by Benettin et al.[9], where counterexamples were given. For a more recent paper [10] Ch. Dellago and H. A. Posch found that there is no simple relationship between the Riemannian curvature along a trajectory and the stability of motion. In a word, the existence of the region of local instability is not a sufficient condition for global instability. Nevertheless, Toda criterion works in many systems [11-14]. We notice that the occurrence of quantum chaotic motion of a single particle in the TCSM is closely related to the shape deformation of a nucleus which actually determines the potential energy surface. Therefore, the study of the local instability determined by the geometry of the potential energy surface may help to understand the dynamical origin of the quantum chaotic motion.

In the present work we shall derive two geometric quantities determining the local Liapunov exponents (the local instability) for the single-particle potential of the TCSM. Our attention will be mainly focused on the connections between the quantum chaotic motion of a single particle in heavy nuclei and the local Liapunov exponents in order to seeking out the dynamical origin of the quantum chaotic motion. Since the neck deformation being a specific feature of the TCSM plays an important role in heavy ion collision, fusion-fission and nuclear molecular states, its influence on the local Liapunov exponents will be particularly paid attention to.

2 The two-center shell model and the chaotic region

Neglecting the spin-orbit coupling and angular momentum square terms, the single-particle Hamiltonian of the TCSM in cylinder coordinates z, ρ, ϕ is as follows

$$H = -\frac{\hbar^2 \nabla^2}{2m_0} + V(\rho, z). \quad (1)$$

The potential reads

$$V(\rho, z) = \begin{cases} \frac{1}{2}m_0\omega_{z_1}^2 z'^2 + \frac{1}{2}m_0\omega_{\rho_1}^2 \rho^2, & z < z_1 \\ \frac{f_0}{2}m_0\omega_{z_1}^2 z'^2 (1 + c_1 z' + d_1 z'^2) \\ \quad + \frac{1}{2}m_0\omega_{\rho_1}^2 (1 + g_1 z'^2)\rho^2, & z_1 < z < 0 \\ \frac{f_0}{2}m_0\omega_{z_2}^2 z'^2 (1 + c_2 z' + d_2 z'^2) \\ \quad + \frac{1}{2}m_0\omega_{\rho_2}^2 (1 + g_2 z'^2)\rho^2, & 0 < z < z_2 \\ \frac{1}{2}m_0\omega_{z_2}^2 z'^2 + \frac{1}{2}m_0\omega_{\rho_2}^2 \rho^2, & z > z_2 \end{cases} \quad (2)$$

by denoting the positions of the centers of the two fragments by z_1 and z_2 , $z_1 \leq 0 \leq z_2$, with the abbreviation

$$z' = \begin{cases} z - z_1, & z < 0 \\ z - z_2, & z > 0 \end{cases}$$

All shape deformation parameters of a nucleus can be reduced to the following five independent ones. (a) The separation of the two centers $\Delta z = z_2 - z_1$. (b) The neck deformation of a nucleus $\epsilon = \frac{E_0}{E'}$, where $E' = \frac{1}{2}m_0\omega_{z_i}^2 z_i^2$ ($i=1,2$), E_0 is the actual height of the barrier [15]. $\epsilon=0$ corresponds to ovaloids, $\epsilon=1$ to well necked-in shapes. (c) The mass asymmetry $X_i = \frac{A_1 - A_2}{A_1 + A_2}$ which ranges from 0 to 1. A_1 and A_2 are the mass numbers of the fragments, which have no explicit expression and are evaluated numerically [15]. (d) The ellipsoidal deformations of the fragments (local deformations) $\beta_i = \frac{\omega_{\rho_i}}{\omega_{z_i}}$ ($i=1,2$). If $X_i = 0$, $\beta_1 = 1 = \beta_2$ and $\epsilon=0$, the shape deformation is a pure quadrupole one. Provided $X_i \neq 0$, an octupole-like deformation appears. If X_i is larger, and local deformations β_1 and β_2 are quite asymmetry (i. e. one of the fragments appears pronounced oblate, the other the pronounced prolate.), then a larger octupole-like deformation is expected.

The parameters in (2) can be written in the form

$$f_0 = 4\epsilon, \quad c_i = \frac{1}{z_i}, \quad d_i = \frac{1}{4z_i^2} \quad (i = 1, 2),$$

$$g_1 = \frac{1 - Q^2}{z_1 \Delta z}, \quad g_2 = \frac{1 - Q^2}{Q^2 z_2 \Delta z},$$

$$z_1 = -\frac{Q_3 \Delta z}{1 + Q_3}, \quad z_2 = \frac{\Delta z}{1 + Q_3}. \quad (3)$$

with $Q = \frac{\omega_{\rho_2}}{\omega_{\rho_1}}$, $Q_3 = \frac{\beta_2}{\beta_1 Q}$. The frequencies ω_{z_i} and ω_{ρ_i} ($i=1,2$) can be determined by the five shape parameters together with the requirements of the volume conservation and smooth joining of the potential. Thus, when the five shape parameters are given all of the parameters in (2) will be determined uniquely.

It has been found that for heavy nuclei the single-particle spacing distribution and spectral rigidity are approximately close to those of GOE when the shape parameters fall into the following region [6]:

$$2.0 < \Delta z < 5.0 \text{ fm}, \quad 0.4 < X_i < 0.7,$$

$$0.2 < \beta_1 < 0.5, \quad 2.0 < \beta_2 < 4.0,$$

$$\epsilon_{min} < \epsilon < 0.9,$$

$$(\epsilon_{min} = 0 \text{ for } 2.0 < \Delta z < 3.0,$$

$$\epsilon_{min} = 0 \sim 0.3 \text{ for } 3.0 < \Delta z < 5.0 \text{ fm}). \quad (I)$$

$$5.0 < \Delta z < 11.0 \text{ fm}, \quad 0.3 < X_i < 0.8,$$

$$0.3 < \beta_1 < 0.6, \quad 2.0 < \beta_2 < 5.0,$$

$$0.3 < \epsilon < 0.8. \quad (II)$$

Both of the parts (I) and (II) of the chaotic region exhibit that the appearance of the quantum chaotic motion requires a considerable octupole-like deformation. The shape parameters in (I) and (II) correspond to the oblate and prolate shapes of a nucleus, respectively. Therefore the quantum chaotic motion occurs not only in the heavy nuclei with oblate shapes but also in prolate ones with a proper neck deformation. The neck deformation appreciably influences the occurrence of the quantum chaotic motion when the separation is medium or large ($5.0 < \Delta z < 11.0$ fm), however it is weakly dependent on ϵ when Δz is small ($2.0 < \Delta z < 5.0$ fm).

3 Local Liapunov exponents and the quantum chaotic motion

Since the single-particle dynamics is connected with the shapes of the potential energy surfaces, an investigation of the effect of the shape deformation on the dynamical behaviour quantitatively requires one to estimate the rate of separation of neighboring trajectories in the phase space. For a Hamiltonian system,

$$H(p, r) = \frac{p^2}{2} + V(r). \quad (4)$$

With the initially neighboring trajectories $r_1(t)$, $p_1(t)$ and $r_2(t)$, $p_2(t)$, the linearized equations of motion for the deviations

$$\xi(t) = r_1(t) - r_2(t), \quad \eta(t) = p_1(t) - p_2(t) \quad (5)$$

have the form

$$\dot{\xi}(t) = \eta(t), \quad \dot{\eta}(t) = -S(t)\xi, \quad (6)$$

where $S(t)$ is the matrix constructed from the second derivatives of potential $V(r)$ and is calculated along the fiducial trajectory $r_1(t)$:

$$S_{ij}(t) = \frac{\partial^2 V}{\partial r_i \partial r_j} \Big|_{r=r_1(t)}. \quad (7)$$

The stability of the motion of the dynamical system in the N - dimension case is described by the $2N \times 2N$ matrix

$$\hat{\Gamma} = \begin{vmatrix} \hat{0} & \hat{I} \\ -\hat{S}(t) & \hat{0} \end{vmatrix},$$

where $\hat{0}$ and \hat{I} are zero and unit $N \times N$ matrices, respectively. One can find a time-dependent transformation \hat{T} such that

$$[\hat{T}\hat{\Gamma}(t)\hat{T}^{-1}]_{ij} = \lambda_i(t)\delta_{ij}. \quad (8)$$

As long as one of the eigenvalues λ_i is real, then the separation of the trajectories grows exponentially, and the motion is unstable. Imaginary eigenvalues correspond to the stable motion. In general, the eigenvalues and, therefore, the nature of the motion, changes with time. To diagonalize the matrix $\hat{\Gamma}(t)$ is equivalent to solving the original equations of the motion. Bolotin assumed [11] that the time-dependent $\hat{S}(t)$ can be eliminated by replacement of the time-dependent point $r_1(t)$ of the phase space by a time-independent coordinate r . This reduces (6) to

$$\dot{\xi} = \eta, \quad \dot{\eta} = -\hat{S}(r)\xi, \quad (9)$$

in which the coordinate r is regarded as a time-independent parameter. The problem is then greatly simplified. For a system with 2 degrees of freedom, the equation for eigenvalues of the matrix $\hat{\Gamma}$ takes the form

$$\det \begin{vmatrix} -\lambda & 0 & 1 & 0 \\ 0 & -\lambda & 0 & 1 \\ -\frac{\partial^2 V}{\partial q_1^2} & -\frac{\partial^2 V}{\partial q_1 \partial q_2} & -\lambda & 0 \\ -\frac{\partial^2 V}{\partial q_1 \partial q_2} & -\frac{\partial^2 V}{\partial q_2^2} & 0 & -\lambda \end{vmatrix}.$$

Its solutions are

$$\lambda_{1,2,3,4} = \pm [-b \pm \sqrt{b^2 - 4c}]^{\frac{1}{2}}, \quad (10)$$

which are called local Liapunov exponents. Here

$$b = S_p S(q) = \frac{\partial^2 V}{\partial q_1^2} + \frac{\partial^2 V}{\partial q_2^2}, \quad (11)$$

$$c = \det \hat{S}(q) = \frac{\partial^2 V}{\partial q_1^2} \frac{\partial^2 V}{\partial q_2^2} - \left(\frac{\partial^2 V}{\partial q_1 \partial q_2} \right)^2. \quad (12)$$

Thus, whether or not the neighboring trajectories in the neighborhood of a point (q_1, q_2) are exponentially separated is simply determined by the presence or absence of a positive local Liapunov exponent λ^+ ($\lambda^+ = [-b + \sqrt{(b^2 - 4c)}]^{\frac{1}{2}}$) which characterizes the local instability. Usually one assumes that $b > 0$, then under the condition that $c > 0$ the solutions are purely imaginary and the motion is stable. For $c < 0$, one pair of roots become real (λ^+ emerges), and this leads to exponential separation of neighboring trajectories. It turns out that c has the same sign as the Gaussian curvature of the potential energy surface [11]. However, in many physical problems b is not always positive. If $b < 0$, then when $c < 0$ or $\frac{b^2}{4} > c > 0$, one can expect a λ^+ . For $c > \frac{b^2}{4}$, the pair of roots become complex (the real part is positive), and this leads to the oscillation of separation of neighboring trajectories with an increasing amplitude with time, thus local instability also takes place.

Now we consider the classical analogy of Hamiltonian (1). In order to be in consistence with (4), the m_0 in (1)-(2) is taken to be 1. According to (11)-(12), the explicit expressions of b and c for the potential described by (2) can be written as

$$b(\rho, z) = \begin{cases} (\omega_{\rho_1}^2 + \omega_{z_1}^2), & z < z_1 \\ \omega_{\rho_1}^2 [(\rho^2 + z'^2)g_1 + 1] \\ \quad + f_0 \omega_{z_1}^2 (1 + 3c_1 z' + 6d_1 z'^2) & z_1 < z < 0 \\ \omega_{\rho_2}^2 [(\rho^2 + z'^2)g_2 + 1] \\ \quad + f_0 \omega_{z_2}^2 (1 + 3c_2 z' + 6d_2 z'^2) & z_2 > z > 0 \\ (\omega_{\rho_2}^2 + \omega_{z_2}^2), & z > z_2, \end{cases} \quad (13)$$

and

$$c(\rho, z) = \begin{cases} \omega_{\rho_1}^2 \omega_{z_1}^2, & z < z_1 \\ \omega_{\rho_1}^4 \rho^2 g_1 (1 - 3g_1 z'^2) + f_0 \omega_{z_1}^2 \omega_{\rho_1}^2 \\ \quad \times (1 + 3c_1 z' + 6d_1 z'^2)(1 + g_1 z'^2) & z_1 < z < 0 \\ \omega_{\rho_2}^4 \rho^2 g_2 (1 - 3g_2 z'^2) + f_0 \omega_{z_2}^2 \omega_{\rho_2}^2 \\ \quad \times (1 + 3c_2 z' + 6d_2 z'^2)(1 + g_2 z'^2) & z_2 > z > 0 \\ \omega_{\rho_2}^2 \omega_{z_2}^2, & z > z_2. \end{cases} \quad (14)$$

By means of (13)-(14), one can see that in the region $z < z_1$ or $z > z_2$ both b and c are positive so that no λ^+ can be obtained in terms of (10). When the shape deformation is pure quadrupole, namely $X_i = 0$, $\beta_1 = 1 = \beta_2$, $\epsilon = 0$ and $g_1 = 0 = g_2$ (in terms of (3)), in the region of $z_1 < z < z_2$ and $0 < \rho < \infty$ the c vanishes and the b is positive. According to (10) a λ^+ will not appear. We find that the typical trajectories in this case are quasi-periodic as shown in Fig.1. So the single-particle motion is stable. However, the negative values of b and c arise in some area in the region $z_1 < z < z_2$, $0 < \rho < \infty$ provided that an octupole-like deformation $X_i \neq 0$ is added. Because of the axial symmetry it is then sufficient just to consider b and

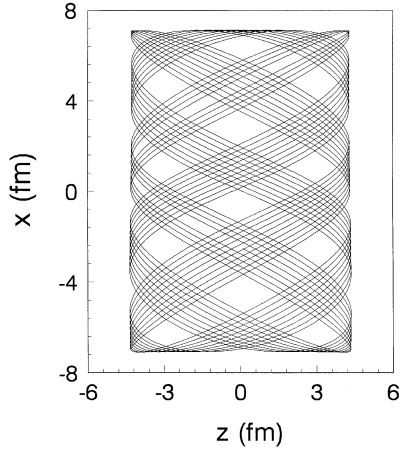


Fig. 1. The typical trajectory in the coordinate space. $\Delta z=9.0$ fm, $X_i=0$, $\beta_1=1=\beta_2$ and $\epsilon=0$. The energy of the system $e=30$ MeV

c in a meridian plane (e. g. x - z plane, a coordinate space). We plot the b and c as functions of x and z in Fig. 2a and Fig. 2b, respectively. One can see that the area with negative values of b and c is located within the region $z_1 < z < z_2$, $-\infty < x < \infty$. According to (10) and the above discussion on the λ^+ , b and c , one can expect the emergence of λ^+ in some area in the region $z_1 < z < z_2$, $-\infty < x < \infty$.

We have found that an octupole-like deformation strongly influences the value of the λ^+ , which, as a function of x and z is displayed for different octupole-like deformations in Fig. 3a-c, where $\Delta z=9.0$ fm, $\epsilon=0.50$, and z is restricted within $z_1 < z < z_2$. In order to examine the relationship between the local and global instabilities of the single-particle system, we also display the typical trajectories characterizing the global instability (or global stability) for each of cases. In Fig. 3a we take $X_i=0.10$,

$\beta_1=0.80$ and $\beta_2=1.20$ (a small octupole-like deformation). One can see that the λ^+ mainly emerges in the vicinity of the point $z=0$, and the area of $|x|>6.0$ fm and $z>0$. The magnitude of the λ^+ is rather small, its maximum is about 10 MeV. In this situation the typical trajectories are no longer quasi-periodic and become rather complicated but less irregular as illustrated in Fig. 3a. With the increase of the octupole-like deformation, the magnitude is increasing. In Fig. 3b, we take $X_i=0.20$, $\beta_1=0.60$ and $\beta_2=1.80$, obviously, the octupole-like deformation is larger than that in Fig. 3a. We find that the magnitude of λ^+ goes up and the area with λ^+ is enlarged compared to that in Fig. 3a, and its maximum value reaches up to 20 MeV. At the same time one can see that the typical trajectory becomes irregular. When an octupole-like deformation is so large that the shape parameters fall into the chaotic region, then the magnitude of λ^+ and the area with λ^+ will become quite large. This is illustrated by Fig. 3c where $X_i=0.40$, $\beta_1=0.40$ and $\beta_2=2.50$ (the five parameters have fallen into the chaotic region), and the maximum value of λ^+ goes up to 40 MeV. As a result, the typical trajectory is extremely irregular (chaotic) in this case.

We notice that when the quantum chaotic motion of the single particle takes place the λ^+ characterizing the locally dynamical instability has a large value in a large area of the coordinate space. Therefore, the occurrence of a large value of λ^+ in a large region of coordinate space should be regarded as the dynamical origin of the quantum chaotic motion. At the same time one can see that the local instability is intimately connected with the global instability of the system and strongly global instability can be realized when the λ^+ has a large value in a large area of the coordinate space. So Toda criterion is valid for the present system.

We find that in the presence of a larger octupole-like deformation, the behaviour of λ^+ does not strongly depend on ϵ when the separation is small (the corresponding shape of a nucleus is oblate). In Fig. 4 the λ^+ versus z

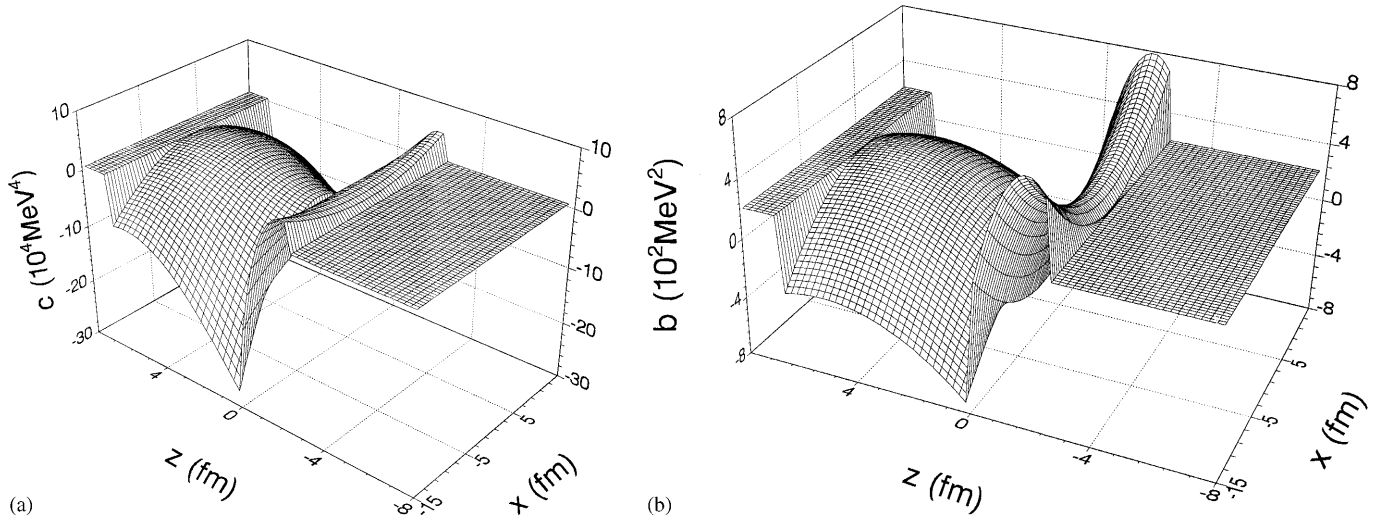


Fig. 2. The b and c as functions of x and z . (a) for b , (b) for c . $\Delta z=9.0$ fm, $\epsilon=0.50$, $X_i=0.40$, $\beta_1=0.40$, $\beta_2=2.50$

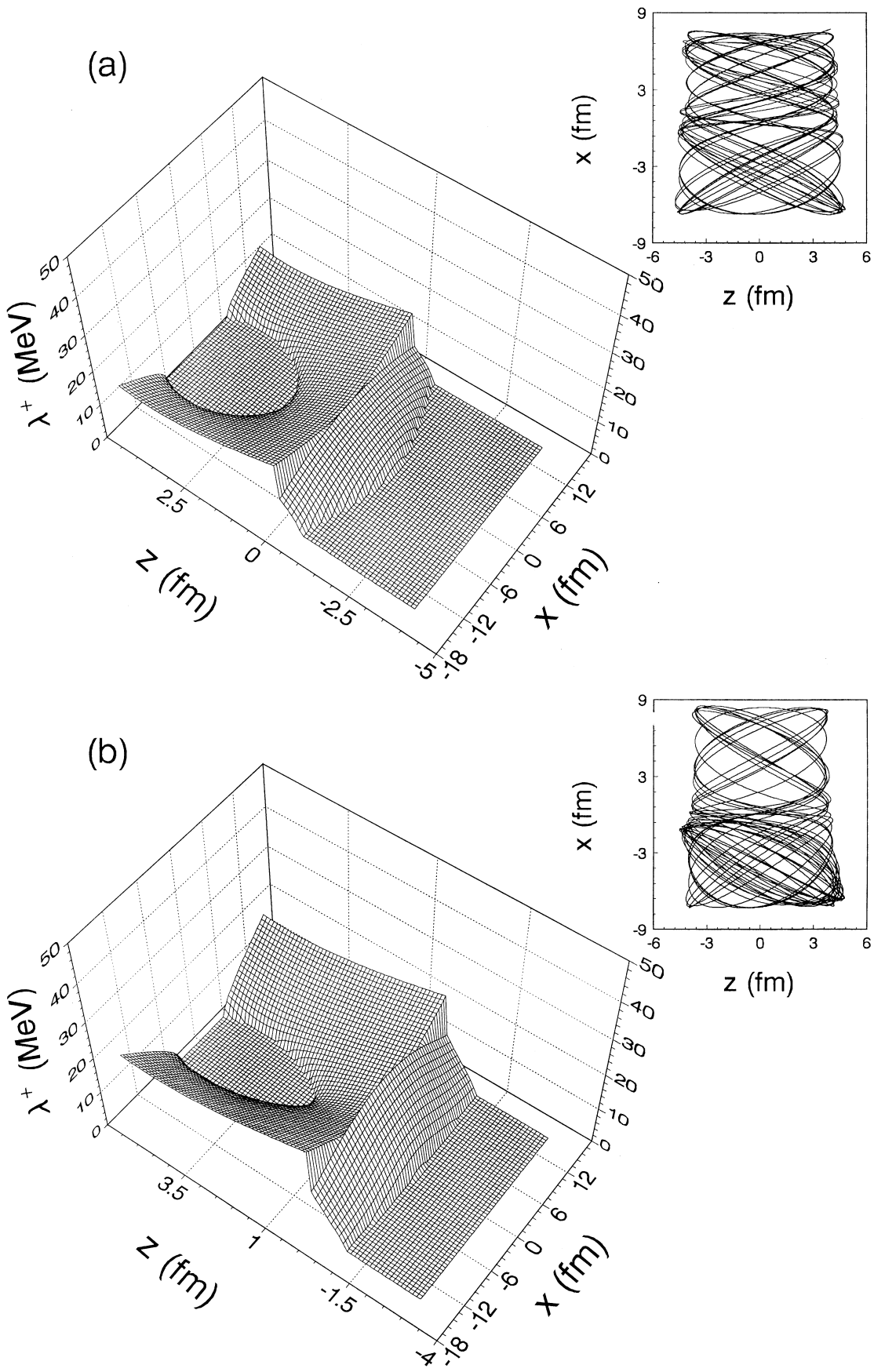


Fig. 3.

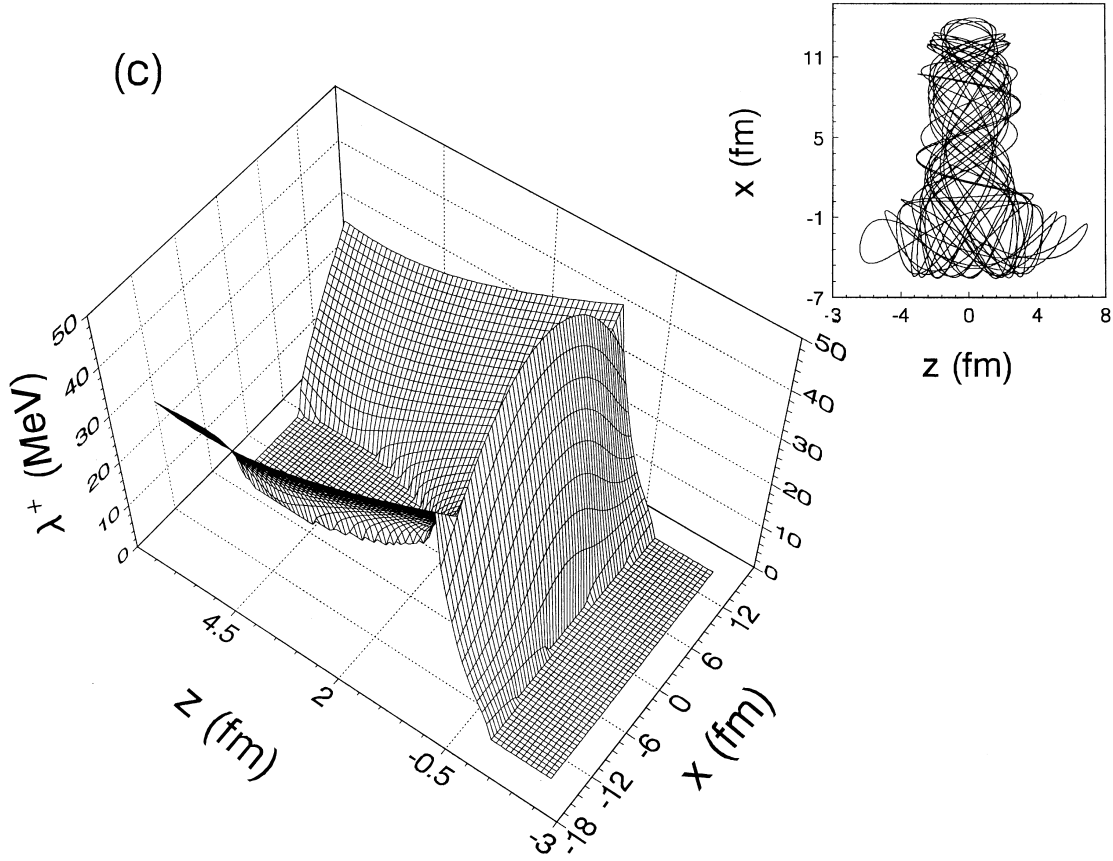


Fig. 3. The λ^+ as a function of x and z for different octupole-like deformations and the corresponding typical trajectories for each of cases, $e=30$ MeV. (a) $\Delta z=9.0$ fm, $\epsilon=0.50$, $X_i=0.10$, $\beta_1=0.80$, $\beta_2=1.20$. (b) $\Delta z=9.0$ fm, $\epsilon=0.50$, $X_i=0.20$, $\beta_1=0.60$, $\beta_2=1.80$. (c) $\Delta z=9.0$ fm, $\epsilon=0.50$, $X_i=0.40$, $\beta_1=0.40$, $\beta_2=2.50$

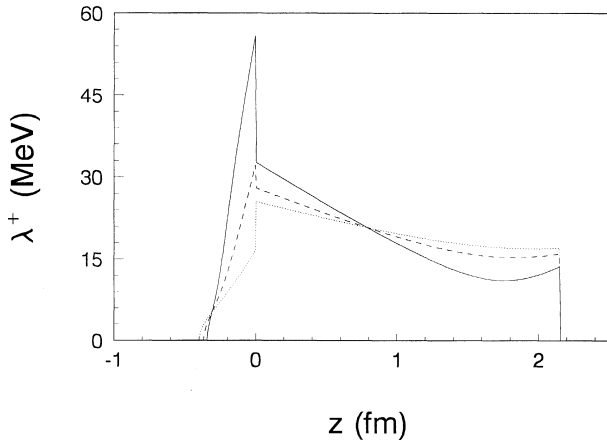


Fig. 4. The λ^+ versus z for different ϵ at a small separation. $\Delta z=3.0$ fm, $X_i=0.40$, $\beta_1=0.40$, $\beta_2=2.50$. The dotted line is for $\epsilon=0.10$, the dashed one for $\epsilon=0.30$, the solid one for $\epsilon=0.60$

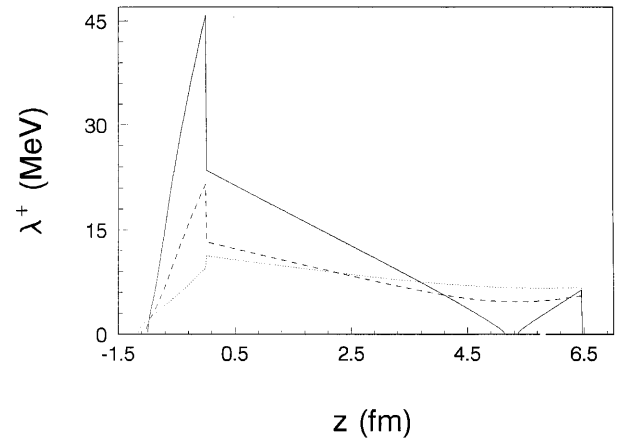


Fig. 5. The λ^+ versus z for different ϵ at a large separation. $\Delta z=9.0$ fm, $X_i=0.40$, $\beta_1=0.40$, $\beta_2=2.50$. The dotted line is for $\epsilon=0.10$, the dashed one for $\epsilon=0.30$, the solid one for $\epsilon=0.60$

at $x=7.0$ fm (such a section can approximately reflect the behavior of λ^+ in the coordinate space) is shown for different ϵ , in which $\Delta z=3.0$ fm, $X_i=0.40$, $\beta_1=0.40$, $\beta_2=2.50$. One can see that the magnitude of the λ^+ is quite large (the maximum is larger than 50 MeV), and the behaviour of the λ^+ is weakly dependent on ϵ . This can be qualita-

tively understood by means of (13)-(14) as follows. When a larger octupole-like deformation is present, the Q in (3) becomes much larger than 1, then g_1 and g_2 also become larger if the separation is small. Thus, the first term of c may have the pronounced negative values in the region $z_2 > z > z_1 + \frac{\sqrt{3}g_1}{3g_1}$. The second term of c becomes neg-

ative in the region $\frac{\sqrt{3}}{3}z_1 < z < \frac{\sqrt{3}}{3}z_2$, its magnitude is determined by ϵ ($f_0 = 4\epsilon$). Therefore, in the presence of a larger octupole-like deformation, a λ^+ with larger magnitude in a larger area can be expected for small separation in the region $\max(z_1 + \frac{\sqrt{3}g_1}{3g_1}, \frac{\sqrt{3}}{3}z_1) < z < \frac{\sqrt{3}}{3}z_2$ even if ϵ is very small. That is the dynamical reason why the quantum chaotic motion weakly depends on ϵ when the separation is small. As the separation is increased, g_1 and g_2 become smaller, the first terms of b and c become smaller too. Then the second term of c becomes indispensable to building a pronounced negative c . Therefore ϵ will appreciably influence the λ^+ , and the occurrence of a large λ^+ in a large area requires a considerable neck deformation in addition to a larger octupole-like deformation. This is corroborated by the following numerical results. In Fig. 5 the λ^+ versus z at $x=7.0$ fm is exhibited for different values of ϵ , in which $\Delta z=9.0$ fm, $X_i = 0.40$, $\beta_1 = 0.40$, $\beta_2=2.50$. One can see that with the increase of ϵ the magnitude of the λ^+ goes up rapidly. Thus it is understood at a dynamical level that why the appearance of the quantum chaotic motion needs a considerable neck deformation when the separation is medium or large. Heiss et al.[3] studied that a single-particle moving in a potential with an octupole deformation built on a quadrupole deformation (neglecting the spin-orbit $l.s$ and square angular momentum l^2 terms). They indicated that the single-particle motion is regular for prolate shapes of nuclei and chaotic for oblate ones. Similar conclusion was drawn also by Arita et al.[4]. In their works, the neck deformation was not included. According to our calculation, for prolate shapes one can not expect the λ^+ with large magnitude in a large area, so that the single-particle quantum chaos can not be induced. However, for oblate shapes the quantum chaotic motion may be induced because the λ^+ with large value may arise in a large area even if the neck deformation is very small.

4 Summary

In the present work we have derived the expressions of b and c which determine the local Liapunov exponents. It has been found an octupole-like deformation strongly influences not only the magnitude of a positive local Liapunov exponent λ^+ but also the area having λ^+ in the coordinate space (x - z plane). The appearance of a large λ^+ in a large area of the coordinate space is the dynamical origin of the quantum chaotic motion of a single particle in heavy nuclei. In the chaotic region of shape parameters the λ^+ can reach a large value in a large area. It has been also shown that the local instability is closely re-

lated to the global instability and Toda criterion is valid for the present system. Meanwhile we have provided the dependence of the quantum chaotic motion for the neck deformation both at small and large (or medium) separations with a dynamical interpretation. In addition, at the dynamical level, it is understood that the single-particle quantum chaotic motion arises only for nuclei with oblate shapes rather than those with prolate ones when a neck deformation is not included. We believe that the present work is heuristic for the study of dynamical origin of the quantum chaotic motion in a general system in which the Hamiltonian is purely governed by its geometry.

We would like to express our gratitude to Prof. Jun-qing Li and Prof. Gong-ou Xu for their useful discussions and suggestions. This work is supported by the National Natural Science Foundation of China and China Postdoctoral Science Foundation.

References

1. T. A. Brody, J. Flores, J. B. French, P. A. Mello, A. Pandey and S. S. M. Wong, Rev. Mod. Phys. 53, 385 (1981); O. Bohigas and H. A. Weidenmüller, Ann. Rev. Nucl. Part. Sci., 38 (1988) 421
2. V. Zelevinsky, B. A. Brown, N. Frazier and M. Horoi, Phys. Rep. 276 (1996) 85
3. W. D. Heiss, R. G. Nazmitdinov and S. Radu, Phys. Rev. Lett. 72 (1994) 2351
4. K. Arita, Phys. Lett. B336 (1994) 279
5. Jian-zhong Gu, Xi-zhen Wu and Yi-zhong Zhuo, Nucl. Phys. A611 (1996) 315; Z. Phys. A354 (1996) 15
6. Jian-zhong Gu, Xi-zhen Wu, Yi-zhong Zhuo and En-guang Zhao, Nucl. Phys. A 625 (1997) 621
7. Jian-zhong Gu, En-guang Zhao, Yi-zhong Zhuo, Xi-zhen Wu and Hong-shi Zong, Eur. Phys. J. A2 (1998) 115
8. M. Toda, Phys. Lett. A48 (1974) 335
9. G. Benettin, R. Brambilla and L. Galgani, Physica 87A (1977) 381
10. Ch. Dellago and H. A. Posch, Physica 230A (1996) 364
11. Y. L. Bolotin, V. Y. Gonchar, E. V. Inopin, V. V. Levenko, V. N. Tarasov and N. A. Chkanov, Sov. J. Part. Nucl. 20 (1989) 372
12. M. Pettini, Phys. Rev. E47 (1993) 828; M. Tabor, Adv. Chem. Phys. 46 (1981) 73
13. Jun-qing Li and Wei-qi Huang, Phys. Rev. C50 (1994) 1632; Jun-qing Li, Jie-ding Zhu and Jin-nan Gu, Phys. Rev. B52 (1995) 6458
14. Jun-qing Li, Phys. Rev. Lett. 79 (1997) 2387; J. Phys. G24 (1998) 1021
15. J. A. Maruhn and W. Greiner, Z. Phys. 251 (1972) 431